10-2015

Dynamics of the transverse Ising model with next-nearest-neighbor interactions

P.R.C. Guimaraes

J.A. Plascak

O.F. de Alcantara Bonfirm
University of Portland

J. Florencio

Dynamics of the transverse Ising model with next-nearest-neighbor interactions

P. R. C. Guimarães[*]
Departamento de Física, Universidade Federal de Viçosa, 36571-000 Viçosa, Minas Gerais, Brazil

J. A. Plascak[†]
Universidade Federal da Paraíba, Centro de Ciências Exatas e da Natureza—Campus I, Departamento de Física, CCEN Cidade Universitária—João Pessoa, PB, Brazil
and Department of Physics and Astronomy, University of Georgia, 30602 Athens, Georgia, USA

O. F. de Alcantara Bonfim[‡]
Department of Physics, University of Portland, Portland, Oregon 97203, USA

J. Florencio[§]
Departamento de Física, Universidade Federal Fluminense, Av. Litorânea s/n, Niterói, 24210-340, RJ, Brazil
(Received 10 July 2015; published 7 October 2015)

We study the effects of next-nearest-neighbor (NNN) interactions on the dynamics of the one-dimensional spin-1/2 transverse Ising model in the high-temperature limit. We use exact diagonalization to obtain the time-dependent transverse correlation function and the corresponding spectral density for a tagged spin. Our results for chains of 13 spins with periodic boundary conditions produce results which are valid in the infinite-size limit. In general we find that the NNN coupling produces slower dynamics accompanied by an enhancement of the central mode behavior. Even in the case of a strong transverse field, if the NNN coupling is sufficiently large, then there is a crossover from collective mode to central mode behavior. We also obtain several recurrants for the continued fraction representation of the relaxation function.

DOI: 10.1103/PhysRevE.92.042115 PACS number(s): 05.70.Ln, 75.10.Pq, 75.10.Jm

I. INTRODUCTION

The dynamical properties of quantum spin systems have been the subject of investigation for the past few decades [1–8]. Recently, there has been an upsurge of interest in spin-1/2 systems, due largely to experiments with ultracold atoms trapped in optical lattices which mimic those systems. Most of the studies in optical lattices are concerned with static properties; however, the dynamical properties of low-dimensional spin-1/2 systems have already been studied in optical lattice settings [9].

The transverse Ising (TI) model stands as one of the simplest quantum spin models with nontrivial spin dynamics. It was introduced in the early 1960s as a theoretical model to study order-disorder transitions in double-well ferroelectric systems such as KH_2PO_4 and its deuterated form KD_2PO_4 (KDP) crystals [10,11] and in PbH PO_4 [12]. The magnetic insulator $LiHoF_4$ is another system that can be described by the TI model [13]. Theoretical efforts have revealed some interesting phenomena in those systems, such as the appearance of central modes, collective modes, anomalous diffusion, etc. Exact results have also been obtained for the dynamical correlation functions in the TI and XY models for one-dimensional (1D) lattices at infinite temperatures [14–17].

Experimental realizations of 1D quantum magnetic chains have been observed in a variety of compounds, tetramethylammonium-manganese-trichloride (TMMC) being a typical example [18,19], as well as some one-dimensional ladder structures such as $(VO)_2P_2O_7$ [20] and $Cu_2(C_5H_{12}N_2)_2Cl_4$ [21]. The magnetic compound $CoNb_2O_6$ is an experimental realization of the TI model that shows a quantum phase transition at zero temperature [22,23]. Recent experiments with ultracold atoms trapped in optical lattices have introduced novel realizations of spin-1/2 systems, such as ferromagnetic Heisenberg quantum magnets [9] and fermionic quantum gases [24–26].

In real magnetic systems the interactions may not be between neighboring spins only. Next-nearest-neighbor (NNN) interactions may play an important role and should be included for a more realistic picture. The model that adds NNN interactions to the TI model is known as the transverse anisotropic next-nearest-neighbor Ising (ANNNI) model [27]. At $T = 0$, this model displays a rich phase diagram with ferromagnetic or antiferromagnetic phases, disordered or paramagnetic phases, and floating phases [28–30].

In the present paper we are interested in the role of the NNN interactions on the dynamics of the transverse ANNNI model. This problem has been studied earlier using the method of recurrence relations [31,32]. The short-time behavior of the time-dependent spin correlation function is well understood. Our numerical method yields results which are valid at much longer times. In addition, our calculations show that the important features of the spectral densities at the thermodynamic limit are already contained in our results.

In the study of spin dynamics, both the time-dependent autocorrelation function and the spectral density play important roles. The latter is related to the experimental crosssection of forward inelastic neutron scattering in real spin systems.

[*]pcolares@ufv.br
[†]pla@physast.uga.edu
[‡]bonfim@up.edu
[§]jfj@if.uff.br

Several approaches have been used to calculate these quantities, including exact diagonalization [33–35] and the method of recurrence relations [8,17,36–38]. The latter has also been applied to electron gases [39], velocity autocorrelation functions of many-body systems [40], and harmonic oscillator chains [41,42].

In the exact diagonalization method, one numerically finds all of the eigenvalues and eigenstates of the Hamiltonian in order to determine the dynamic correlation functions of the system. Since the number of states increases exponentially with the size of the system L, numerical efforts are limited to systems with relatively small sizes. Even with such restrictions, these methods have produced reliable results when compared with known exact results.

On the other hand, the method of recurrence relations produces analytic results for the dynamic correlation functions of interest. There are a few instances where the recurrence relations method produces exact results, such as in the TI and XY models [17], as well as in harmonic oscillator chains [41,42]. It does not require explicit knowledge of the eigenvalues and eigenstates of the Hamiltonian. However, one must determine the recurrants, which are essential to the method. They are the coefficients of a continued fraction representation of the Laplace transform of the correlation function [7,8].

The analytical calculation of the recurrants is usually very time-consuming, and, consequently, only a few of them are obtained in general. In those cases, the time-dependent correlation function is written as a short-time expansion. In order to extend the time domain, more recurrants are needed. Often one needs to devise a termination procedure for the continued fraction. Several approaches along this line have been used in the literature [1,5,6,43–46]. Given that the known exact recurrants are needed to form the basis of the termination scheme, the knowledge of as many recurrants as possible is a desirable condition for the construction of a reliable approximation to the continued fraction representation of the dynamic correlation functions.

This paper is organized as follows. In Sec. II we present the model and give a review of the method of exact diagonalization. In Sec. III we present a short account of the method of recurrence relations. In Sec. IV we discuss our results for the dynamical correlation functions. In Sec. V we show our numerical results for the recurrants of the method of recurrencer relations, and, finally, we summarize our findings in Sec. VI.

II. MODEL AND EXACT DIAGONALIZATION

The spin-1/2 transverse ANNNI model for a chain of L spins is defined by the Hamiltonian:

$$H = -J\sum_{i=1}^{L}\sigma_i^x\sigma_{i+1}^x - J_2\sum_{i=1}^{L}\sigma_i^x\sigma_{i+2}^x - B\sum_{i=1}^{L}\sigma_i^z, \quad (1)$$

where σ_i^α, $\alpha = x,y,z$, are Pauli matrices; J and J_2 are the energy couplings between first- and second-neighbor spins, respectively; B is the energy coupling of a spin in a transverse magnetic field; and periodic boundary conditions are assumed, namely $\sigma_{i+L}^\alpha = \sigma_i^\alpha$. Notice that our definition of the coupling energies implies that in the absence of NNN interactions the quantum phase transition ($T = 0$) occurs when $B/J = 1$.

The time-dependent transverse correlation function of a tagged spin at site j is defined as

$$C(t) = \langle\sigma_j^x(0)\sigma_j^x(t)\rangle, \quad (2)$$

where $\sigma_j^x(t) = \exp(iHt)\sigma_j^x\exp(-iHt)$, $\hbar = 1$, and the brackets denote a canonical average. At the infinite-temperature limit ($T = \infty$) all states contribute with the same statistical weight. The correlation function is given by

$$C(t) = \frac{1}{2^L}\mathrm{Tr}\left(\sigma_j^x e^{iHt}\sigma_j^x e^{-iHt}\right). \quad (3)$$

Here $C(t)$ is both real and even in t. Also, its time derivative is zero at $t = 0$. Its Taylor expansion about $t = 0$ can be written as

$$C(t) = \sum_{k=0}^{\infty}\frac{(-1)^k}{(2k)!}\mu_{2k}\,t^{2k}. \quad (4)$$

The moments μ_{2k} are defined in terms of a trace over iterated commutators,

$$\mu_{2k} = \frac{1}{2^L}\mathrm{Tr}\left(\sigma_j^x\mathcal{L}^{2k}\sigma_j^x\right), \quad (5)$$

where $\mathcal{L}$ is the Liouville operator,

$$\mathcal{L}A = [H,A] = HA - AH, \quad (6)$$

A is an operator, and H is the Hamiltonian.

In terms of the energies and eigenstates of the Hamiltonian, $H|n\rangle = E_n|n\rangle$, the correlation function assumes the form:

$$C(t) = \frac{1}{2^L}\sum_{m,n}\cos(E_n - E_m)t\,|\langle n|\sigma_j^x|m\rangle|^2. \quad (7)$$

The moments are now given by

$$\mu_{2k} = \frac{1}{2^L}\sum_{m,n}(E_n - E_m)^{2k}|\langle n|\sigma_j^x|m\rangle|^2. \quad (8)$$

Another quantity of interest is the spectral density $S(\omega)$, given by the time Fourier transform of $C(t)$,

$$S(\omega) = \int_{-\infty}^{\infty}C(t)e^{-i\omega t}dt. \quad (9)$$

By using Eq. (7) the spectral density reads

$$S(\omega) = \frac{\pi}{2^L}\sum_{m,n}|\langle n|\sigma_j^x|m\rangle|^2[\delta(\omega - \epsilon_{nm}) + \delta(\omega + \epsilon_{nm})], \quad (10)$$

where $\epsilon_{nm} \equiv E_n - E_m$.

In our numerical calculations, the Dirac δ functions are approximated by rectangles of width a and unit area, centered at the zeros of their arguments. The width a can be adjusted to reduce fluctuations. However, that does not change the general shape of the spectral density $S(\omega)$. Numerical evaluation of the eigenstates and eigenvalues of the Hamiltonian allows us to directly evaluate both the time-dependent correlation function, Eq. (7), and the spectral density, Eq. (10).

III. METHOD OF THE RECURRENCE RELATIONS

The time evolution of an operator A in the Heisenberg representation, $A(t) = \exp(iHt)A\exp(-iHt)$, in a system governed by a Hamiltonian H, is cast as the expansion

$$A(t) = \sum_{\nu=0}^{d-1} c_\nu(t) f_\nu, \tag{11}$$

where f_ν's are orthogonal basis vectors spanning a d-dimensional Hilbert space $\mathcal{S}$. In general, these vectors are not normalized. In the infinite-temperature limit, the scalar product in $\mathcal{S}$ can be defined by

$$(A, B) = \frac{1}{Z}\mathrm{Tr}\, AB^\dagger, \tag{12}$$

where Z is the canonical partition function.

Consider the time evolution of a tagged spin at site j. Thus we set $A(t) \equiv \sigma_j^x(t)$ in Eq. (11) and choose the basal vector $f_0 = \sigma_j^x$. It follows that the time-dependent coefficient $c_o(t) = C(t)$, the time-dependent spin correlation function, Eq. (2). The remaining basis vectors are obtained recursively by the recurrence relation (RRI):

$$f_{\nu+1} = i\mathcal{L}f_\nu + \Delta_\nu f_{\nu-1}, \qquad \nu \geqslant 0, \tag{13}$$

with $\mathcal{L}$ defined in Eq. (6), $\Delta_0 \equiv 1$, $f_{-1} \equiv 0$, and

$$\Delta_\nu = \frac{(f_\nu, f_\nu)}{(f_{\nu-1}, f_{\nu-1})}, \qquad \nu \geqslant 1, \tag{14}$$

are called recurrants, which are obtained from the ratio of the norms of the basis vectors in $\mathcal{S}$. Therefore they are positive definite.

The time-dependent coefficients $c_\nu(t)$ are determined from the second recurrence relation (RRII):

$$\Delta_{\nu+1}c_{\nu+1}(t) = -\frac{dc_\nu(t)}{dt} + c_{\nu-1}(t), \quad 0 \leqslant \nu \leqslant d-1, \tag{15}$$

where $c_{-1}(t) \equiv 0$. According to RRII, the time dependence is determined entirely from the Δ_ν's, hence the importance of accurate and reliable knowledge of them. The recurrants can be used for the characterization of infrared singularities in spectral densities [46]. Furthermore, they can help to understand how correlation functions of very different systems may sometimes exhibit the very same time dependence [47].

To proceed further, it is convenient to obtain the Laplace transform of RRII,

$$\Delta_1 a_1(z) = 1 - a_0(z), \tag{16}$$

$$\Delta_{\nu+1}a_{\nu+1}(z) = -z\, a_\nu(z) + a_{\nu-1}(z), \quad n \geqslant 1, \tag{17}$$

where

$$a_\nu(z) = \int_0^\infty c_\nu(t)\mathrm{e}^{-zt}dt, \quad \mathrm{Re}(z) > 0. \tag{18}$$

In particular, $a_0(z)$, also known as the relaxation function, is defined by:

$$a_0(z) = \int_0^\infty C(t)\mathrm{e}^{-zt}dt, \quad \mathrm{Re}(z) > 0. \tag{19}$$

It follows from Eqs. (16) and (17) that $a_0(z)$ can assume the form of a continued fraction,

$$a_0(z) = \cfrac{1}{z + \cfrac{\Delta_1}{z + \cfrac{\Delta_2}{z + \cdots}}}. \tag{20}$$

The spectral density $S(\omega)$ can be obtained from $a_0(z)$ by using the relation

$$S(\omega) = \lim_{\epsilon \to 0^+} \mathrm{Re}[2a_0(\epsilon - i\omega)]. \tag{21}$$

There are also conversion formulas connecting the recurrants to the moments [6]. Without loss of generality we set $\mu_0 = 1$, which is consistent with the normalized time-dependent correlation function defined in Eq. (2). Once the the first moments are known up to order $2k$, the conversion formulas yield the first k recurrants $\Delta_1, \ldots, \Delta_k$. Then one obtains $\Delta_1 = \mu_2$, $\Delta_2 = -\mu_2 + \mu_4/\mu_2$, $\Delta_3 = (\mu_4^2/\mu_2 - \mu_6)/(\mu_2^2 - \mu_4)$, etc.

IV. RESULTS FOR THE DYNAMICAL CORRELATION FUNCTIONS

Consider first the TI model defined in Eq. (1) with $B = 1$ and $J_2 = 0$. In this case the dynamical correlation functions for the infinite system are known exactly in the high-temperature limit [16,17]. Figure 1 shows our numerical results for the time-dependent correlation function for $B = 1$ and several lattice sizes. The results agree very well with the exact result of the infinite system, $C(t) = \exp(-2J^2t^2)$. Notice the logarithmic scale for $C(t)$, which magnifies the differences between the numerical finite chain results and the known exact result. The region of agreement between infinite and finite chains is extended as L increases. For example, the smallest size shown $L = 9$ agrees very well up to $t = 3.3$, whereas the largest size $L = 13$ is very close to the exact result up to approximately $t = 4.1$. The discrepancy is about one part in 10^{14} for longer times.

The corresponding spectral densities are depicted in Fig. 2, which shows our results for finite chains and the exact Gaussian result $S(\omega) = \sqrt{\pi/2J^2}\exp(-\omega^2/8J^2)$ for $L = \infty$.

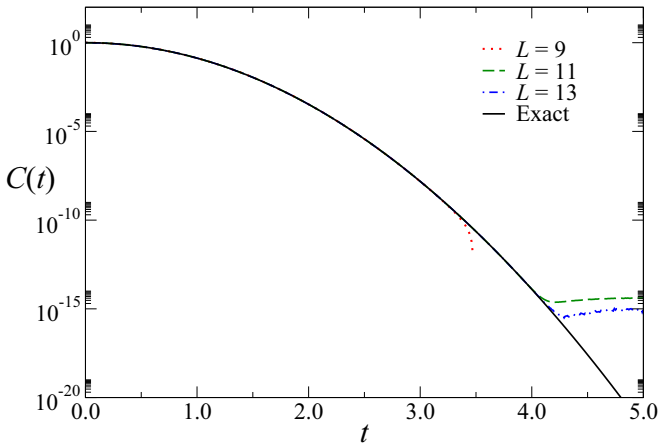

FIG. 1. (Color online) Time-dependent transverse correlation function of a tagged spin in the TI model when $B = J = 1.0$ for chain sizes $L = 9, 11$, and 13, together with the known Gaussian result of the infinite chain. Here and in the next figures we use $J = 1$ as the unit of energy.

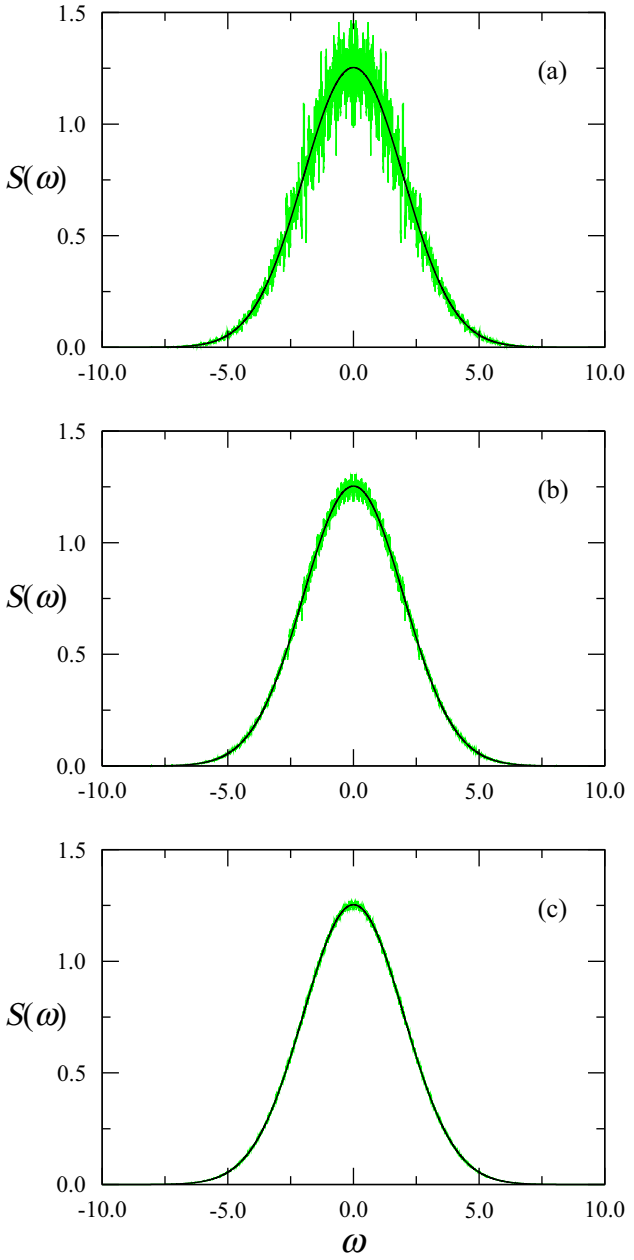

FIG. 2. (Color online) Spectral density for the TI model for $B = 1$ and several chain sizes, (a) $L = 9$, (b) $L = 11$, and (c) $L = 13$. The solid line is the exact Gaussian result for the infinite system.

Notice that the curve for $L = 13$ shows excellent agreement throughout the frequency range. Throughout the paper we use $J = 1$ as the unit of energy.

Our results were obtained by using Eq. (10), where we approximate the Dirac δ functions by a rectangle of unit area and width $a = 0.1$. Smaller values of the parameter a, would simply increase the fluctuation of $S(\omega)$ about the exact Gaussian result. One should note that even for smaller lattices such as $L = 9$ and 11, the curves nearly reproduce the exact Gaussian result, albeit showing larger fluctuations. These fluctuations become smaller as the lattice size increases. In this way, $S(\omega)$ for small lattice sizes already convey the essential quantitative features of the infinite system.

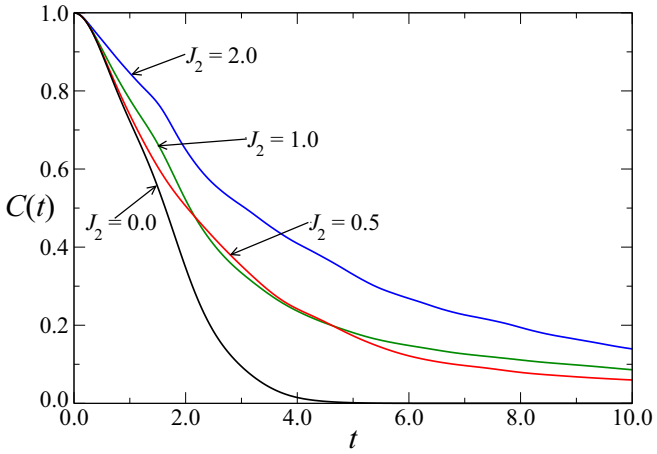

FIG. 3. (Color online) Time-dependent correlation function for $B = 0.5$ and several values of the NNN coupling J_2. Each curve is the overlap of two curves: one obtained for $L = 12$ and other for $L = 13$.

We now turn to the transverse ANNNI model. Our calculations were done in the high-temperature limit. We consider the cases $B = 0.5$, $B = 1.0$, and $B = 2.0$, which are representative values of the energy couplings of the TI model.

We first consider the influence of NNN interactions for the case $B = 0.5$. In Fig. 3, the time-dependent correlation function is plotted for several values of J_2. The curves were obtained for the chain sizes $L = 12$ and 13. They agree very well with each other in the time interval displayed in the figure. Results will not change noticeably in the scale of the figure if we use larger lattices. Hence we believe we have achieved thermodynamic limit results with relatively small lattices (up to $L = 13$). We can see from the figure that the relevant structures in $C(t)$ are already displayed in our results for finite-sized lattices. The wavering on the curves of $C(t)$ for the cases $J_2 = 0.5$, 1.0, and 2.0 as well as the two crossings between the plots for $J_2 = 0.5$ and 1.0 are real and will not change for larger systems. These results will remain unchanged

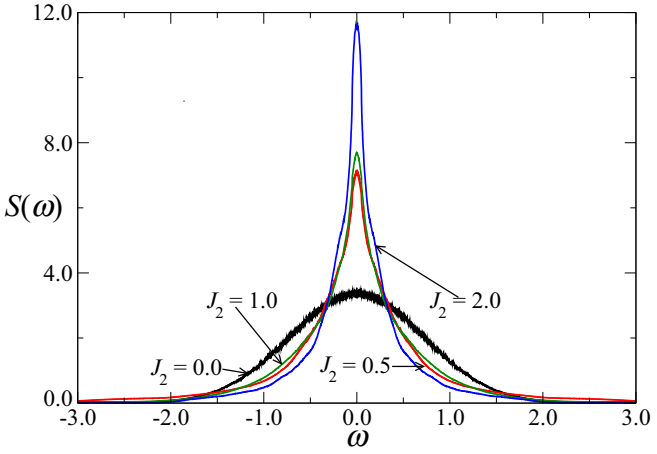

FIG. 4. (Color online) Spectral density for $B = 0.5$ and several values of J_2. All the curves were obtained for chains with $L = 13$.

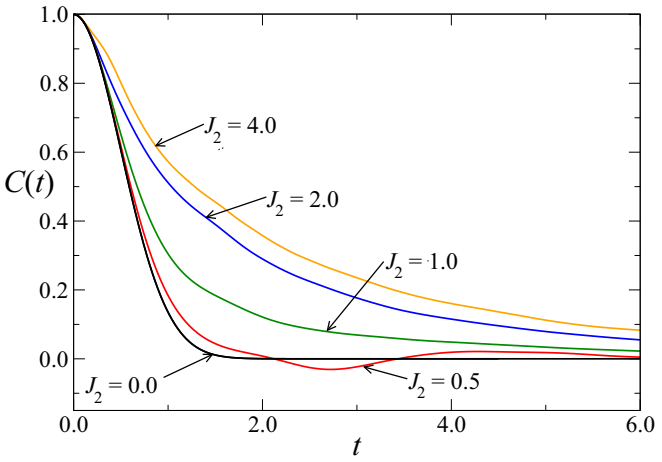

FIG. 5. (Color online) Time-dependent correlation function for $B = 1$ and several values of J_2. The curves were obtained with $L = 12$ and 13.

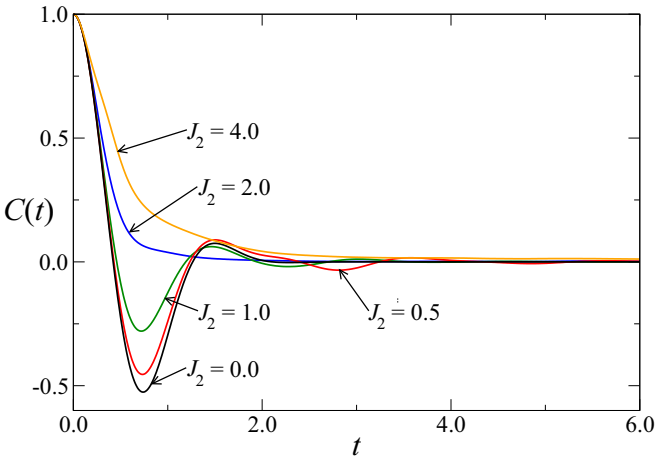

FIG. 7. (Color online) Time-dependent correlation function for $B = 2.0$ and various values of J_2. The curves were obtained for chain sizes $L = 12$ and 13.

for systems at the thermodynamic limit. Our results show that $C(t)$ decays at slower rates as J_2 increases.

The spectral density is depicted in Fig. 4, which was obtained for a chain of $L = 13$. Smaller-sized lattices produce essentially the same results, but with larger oscillations. Those oscillations are a finite-size effect and do not survive in the thermodynamic limit. When $J_2 = 0$, central mode behavior dominates the dynamics. For larger values of J_2 there is an enhancement of the central peak, with a rise of its height around $\omega = 0$ accompanied by a narrowing of the curve. In these cases NNN interactions foster central mode behavior.

The case $B = 1.0$ and $J_2 = 0$ corresponds to the TI model at criticality ($T = 0$) [22]. In Fig. 5 the time-dependent correlation function $C(t)$ is shown for some values of J_2. For $J_2 = 0.5$ the decay of $C(t)$ becomes slower as compared to that of the TI model. However, an oscillation appears, approximately between $2.0 \leqslant t \leqslant 4.0$, and then the correlation function goes steadily toward zero as t increases. As we consider higher values of J_2 the rate of decay becomes slower, with suppression of the oscillation present when $J_2 = 0.5$. For larger values of J_2 the oscillations in $C(t)$ disappear entirely and the time decay is slower. The corresponding spectral densities are depicted in Fig. 6. When $J_2 = 0$ we obtain the known Gaussian result. However, for $J_2 = 0.5$, two small shoulders appears around $\omega = \pm 1$. For $J_2 = 1.0$ the shoulders disappear altogether and

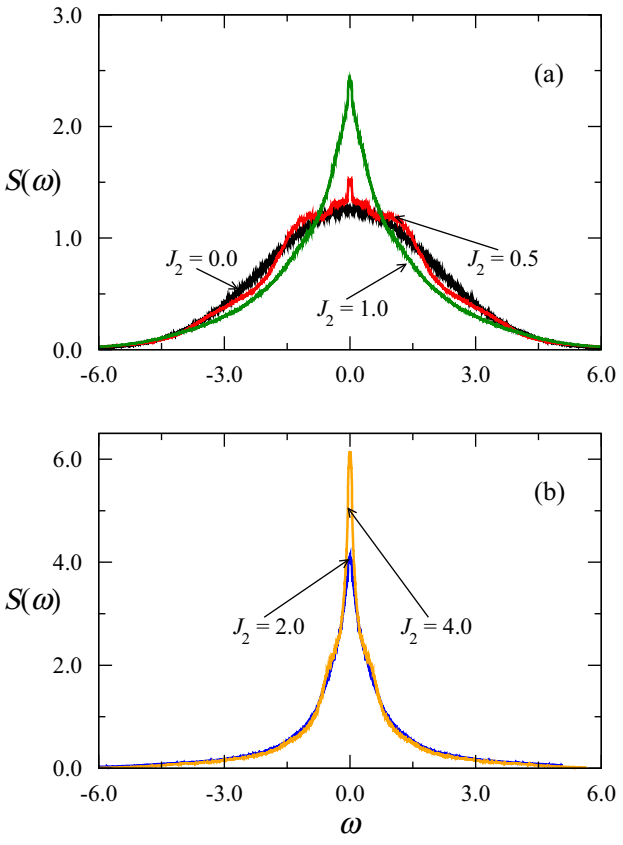

FIG. 6. (Color online) Spectral density for $B = 1$ and several values of J_2, obtained for chains of length $L = 13$. The vertical scales of (a) and (b) were chosen to show more clearly the details of each of the curves.

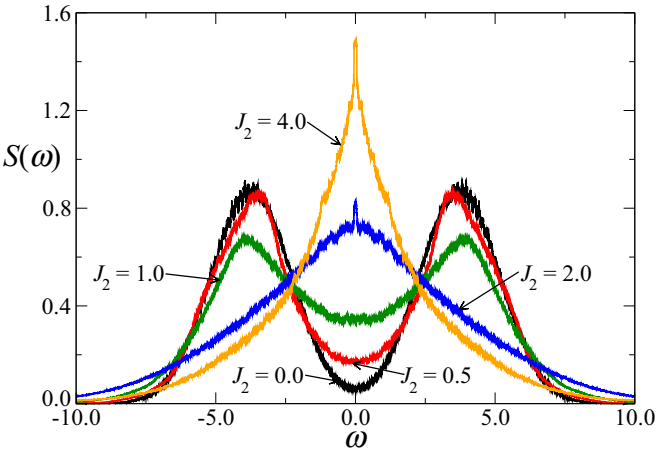

FIG. 8. (Color online) Spectral density for the case $B = 2$ and several values of J_2. The plots were obtained for chains of size $L = 13$.

TABLE I. Recurrants for the transverse ANNNI model, with $B = 1.0$, $J_2 = 1.0$, and several chain sizes.

Δ_ν	$L = 11$	$L = 12$	$L = 13$	$L = \infty$
Δ_1	4.00000	4.00000	4.00000	4.00000
Δ_2	16.0000	16.0000	16.0000	16.0000
Δ_3	28.0000	28.0000	28.0000	28.0000
Δ_4	41.1429	41.1429	41.1429	41.1429
Δ_5	51.3016	51.3016	51.3016	51.3016
Δ_6	73.0933	73.0933	73.0933	73.0933
Δ_7	78.5228	78.5228	78.5228	78.5228
Δ_8	92.4927	92.4927	92.4927	92.4927
Δ_9	110.406	110.406	110.406	110.406
Δ_{10}	127.334	127.334	127.334	127.334
Δ_{11}	151.014	151.014	151.014	151.014
Δ_{12}	168.388	168.385	168.385	168.385
Δ_{13}	191.746	191.673	191.672	191.67
Δ_{14}	216.807	216.023	215.961	216.0
Δ_{15}	233.220	229.579	229.217	2.3×10^2
Δ_{16}	269.065	259.252	258.141	2.6×10^2
Δ_{17}	298.445	281.726	278.903	2.8×10^2
Δ_{18}	336.633	312.762	305.475	3×10^2

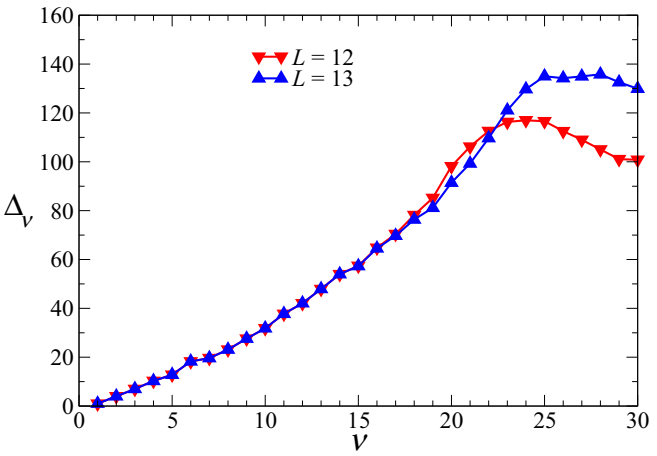

FIG. 9. (Color online) Recurrants for $B = J_2 = 1.0$ and chain sizes $L = 12$ and 13.

there is a sharp increase of the central peak around $\omega = 0$. Again, central mode behavior becomes dominant.

Finally, we consider the case $B = 2.0$. The time-dependent correlation function is shown in Fig. 7 for several NNN interaction energies J_2. For small NNN couplings the dynamics

TABLE II. Recurrants for the transverse ANNNI model for $B = 0.5$ and several NNN couplings at the thermodynamic limit.

Δ_ν	$J_2 = 0.0$	$J_2 = 0.5$	$J_2 = 1.0$	$J_2 = 2.0$	$J_2 = 4.0$
Δ_1	1.00000	1.00000	1.00000	1.00000	1.00000
Δ_2	8.00000	10.0000	16.0000	40.0000	136.000
Δ_3	9.00000	14.2000	25.0000	53.8000	152.059
Δ_4	5.33333	16.1239	28.8000	50.4268	71.8116
Δ_5	11.6667	21.0443	28.3778	52.7022	185.597
Δ_6	10.2857	31.3921	46.8047	79.3706	129.162
Δ_7	12.0476	34.7908	74.3243	161.212	303.648
Δ_8	23.3149	42.0656	44.2156	158.841	677.005
Δ_9	25.6176	52.0678	74.9213	92.9177	314.612
Δ_{10}	28.6558	59.7696	90.0865	139.676	273.028
Δ_{11}	20.9597	69.1325	107.447	185.526	258.917
Δ_{12}	25.0746	76.1694	104.371	186.036	508.166
Δ_{13}	32.5912	84.4063	107.801	258.059	480.341
Δ_{14}	28.7291	9.707×10	1.672×10^2	1.7394×10^2	563.317
Δ_{15}	29.4130	1.083×10^2	1.53×10^2	3.800×10^2	462.216
Δ_{16}	2.9875×10	1.15×10^2	1.6×10^2	3.602×10^2	7.1686×10^2
Δ_{17}	3.772×10	1.3×10^2	1.7×10^2	3.49×10^2	1.4118×10^3
Δ_{18}	3.55×10	1.4×10^2	2.2×10^2	2.87×10^2	8.243×10^2
Δ_{19}	4.2×10	2×10^2	2×10^2	4.3×10^2	1.021×10^3
Δ_{20}	6×10	2×10^2	2×10^2	5.7×10^2	6×10^2
Δ_{21}		2×10^2		4.9×10^2	
Δ_{22}		2×10^2		5×10^2	
Δ_{23}		2×10^2		4×10^2	
Δ_{24}		2×10^2		6×10^2	
Δ_{25}		2×10^2		6×10^2	
Δ_{26}		2×10^2		8×10^2	
Δ_{27}		2×10^2		7×10^2	
Δ_{28}		2×10^2			
Δ_{29}		2×10^2			
Δ_{30}		2×10^2			
Δ_{31}		2×10^2			

TABLE III. Recurrants for the transverse ANNNI model with $B = 1.0$ and several NNN couplings at the thermodynamic limit.

Δ_v	$J_2 = 0.0$	$J_2 = 0.5$	$J_2 = 1.0$	$J_2 = 2.0$	$J_2 = 4.0$
Δ_1	4.00000	4.00000	4.00000	4.00000	4.00000
Δ_2	8.00000	10.0000	16.0000	40.0000	136.000
Δ_3	12.0000	17.2000	28.0000	56.8000	155.059
Δ_4	16.0000	27.1256	41.1429	64.4958	87.9579
Δ_5	20.0000	38.1134	51.3016	79.4813	209.873
Δ_6	24.0000	45.0486	73.0933	132.517	209.281
Δ_7	28.0000	52.3881	78.5228	173.651	454.794
Δ_8	32.0000	68.9177	92.4927	172.678	600.475
Δ_9	36.0000	80.7347	110.406	160.869	321.680
Δ_{10}	40.0000	88.8777	127.334	207.220	393.603
Δ_{11}	44.0000	108.274	151.014	240.888	411.160
Δ_{12}	48.0000	116.218	168.385	283.646	678.810
Δ_{13}	52.0000	138.065	1.9167×10^2	306.446	516.472
Δ_{14}	56.0000	1.463×10^2	2.160×10^2	3.958×10^2	663.910
Δ_{15}	60.0000	1.64×10^2	2.3×10^2	4.465×10^2	1013.41
Δ_{16}	64.0000	1.84×10^2	2.6×10^2	4.1×10^2	1258.29
Δ_{17}	6.8×10	1.9×10^2	2.8×10^2	4.8×10^2	1019.40
Δ_{18}	7.2×10	2×10^2	3×10^2	5.6×10^2	1.001×10^3
Δ_{19}	7.6×10	2×10^2	3×10^2	6.3×10^2	1.25×10^3
Δ_{20}	8.0×10	3×10^2	4×10^2	6×10^2	1.81×10^3
Δ_{21}		3×10^2	4×10^2	6×10^2	2.021×10^3
Δ_{22}		3×10^2			1.213×10^3
Δ_{23}		3×10^2			1.4×10^3
Δ_{24}					1.6×10^3
Δ_{25}					2×10^3

TABLE IV. Recurrants of the transverse ANNNI model for $B = 2.0$ and several NNN couplings at the thermodynamic limit.

Δ_v	$J_2 = 0.0$	$J_2 = 0.5$	$J_2 = 1.0$	$J_2 = 2.0$	$J_2 = 4.0$
Δ_1	16.0000	16.0000	16.0000	16.0000	16.0000
Δ_2	8.00000	10.0000	16.0000	40.0000	136.000
Δ_3	24.0000	29.2000	40.0000	68.8000	167.059
Δ_4	32.0000	48.5260	72.0000	108.502	146.744
Δ_5	80.0000	98.5757	112.711	143.235	265.255
Δ_6	56.0000	79.5622	114.557	194.311	344.992
Δ_7	53.7143	92.3654	140.778	241.101	539.695
Δ_8	65.9453	141.023	187.668	274.712	640.982
Δ_9	87.4673	181.068	208.883	302.936	516.588
Δ_{10}	63.5371	180.048	234.620	343.635	604.328
Δ_{11}	86.4555	198.269	267.206	400.984	675.242
Δ_{12}	103.953	208.378	306.764	469.974	8.4865×10^2
Δ_{13}	122.743	289.404	3.6132×10^2	5.4070×10^2	8.8739×10^2
Δ_{14}	158.820	3.1198×10^2	3.972×10^2	6.1×10^2	1.229×10^3
Δ_{15}	175.134	3.204×10^2	4.35×10^2	6.7×10^2	1.405×10^3
Δ_{16}	131.441	3.76×10^2	4.7×10^2	7.3×10^2	1.340×10^3
Δ_{17}	1.5046×10^2	3.56×10^2	5.1×10^2	8.0×10^2	1.46×10^3
Δ_{18}	1.60×10^2	4.3×10^2	6×10^2	8.0×10^2	1.77×10^3
Δ_{19}	1.8×10^2	4.0×10^2	6×10^2	9×10^2	2.1×10^3
Δ_{20}	2×10^2	5×10^2	7×10^2	9×10^2	2.0×10^3
Δ_{21}				1×10^3	2×10^3
Δ_{22}				1×10^3	2×10^3
Δ_{23}				1×10^3	
Δ_{24}				1×10^3	

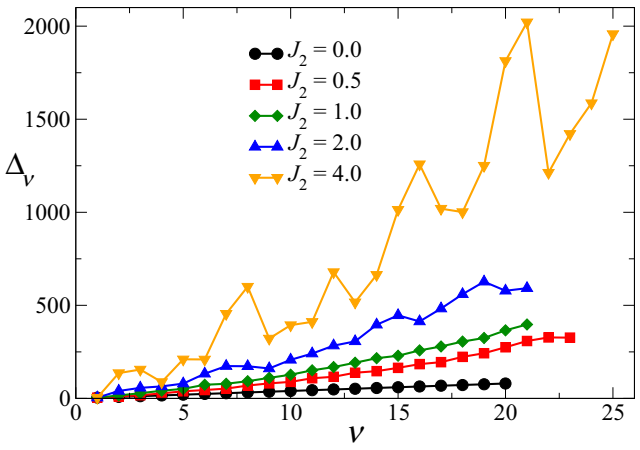

FIG. 10. (Color online) Recurrants of the infinite transverse ANNNI model with $B = 1.0$ and several values of J_2 (data taken from Table III).

is dominated by the collective mode with well-defined oscillatory behavior. As J_2 increases, a crossover from collective to central mode behavior takes place. This is best seen in Fig. 8, which shows the spectral function. The crossover occurs, approximately, in the range $1.0 < J_2 < 2.0$.

V. NUMERICAL EVALUATION OF THE RECURRANTS

In the spin-1/2 transverse ANNNI model in 1D at infinite temperature, the first 5 analytic results [31] and the first 9 numerical results [32] for the recurrants are known. By using exact diagonalization we obtain between 18 and 31 recurrants with varying degrees of accuracy.

In Table I we report our numerical results for $B = J_2 = 1.0$ and system sizes $L = 11$, 12, and 13. The first recurrants for these lattice sizes have already converged to their thermodynamic values ($L = \infty$), which are displayed in the last column. For $\nu \geqslant 13$, there is a gradual reduction in the accuracy of the thermodynamic recurrants, such that the highest-order reported, Δ_{18}, contains only a single significant digit. Figure 9 shows the results from exact diagonalization given in Table I for $L = 12$ and 13.

Our main results for the recurrants are presented in Tables II, III, and IV for the cases $B = 0.5$, $B = 1.0$, and $B = 2.0$, respectively. These are already the values of the recurrants for infinite systems, free from finite-size effects.

In Fig. 10 we show the recurrants for the case $B = 1.0$ and several NNN couplings. The case $J_2 = 0$ reproduces the known result of the TI model, with linear dependence of Δ_ν with ν. In our numerical work with $L = 13$ spins, we obtain the first 20 exact or near exact recurrants. One of the effects of increasing J_2 is that the recurrants increase at a higher rate, on the average. In addition, no clear pattern can be inferred from the first recurrants shown in the figure. It may prove very difficult to devise a reliable extrapolation scheme for large values of J_2, especially due to the seemingly erratic oscillations of the Δ's in those cases. In the case $J_2 = 4.0$, a power-law fit using the data of the figure yields $\Delta_\nu \sim \nu^{1.5}$, which is slower than a quadratic growth, with its known problems associated with the convergence of the continued fractions, as discussed by Sen [48]. As can be seen in Figs. 5 and 6(b), both time-dependent correlation function and the spectral density for that case are obtained without any problems by using the method of exact diagonalization. Furthermore, as we saw earlier, direct results from exact diagonalization of a chain with size $L = 13$ already provide a good quantitative picture for the dynamic correlation functions of the infinite system ($L \to \infty$).

VI. SUMMARY

We have studied the dynamics of the 1D transverse ANNNI model at the high temperature limit by using exact diagonalization of finite chains. We determined the time-dependent spin correlation function and the associated spectral density for chains with sizes up to $L = 13$ with periodic boundary conditions. Our results closely approximate to the exact thermodynamic ones and are free from finite-size effects. NNN couplings produce slower time decays for the correlation functions, as well as an enhancement in the central mode behavior. For the case where the applied transverse field is sufficiently large, an increase in the NNN coupling produces a crossover from collective mode (dominated by the transverse field) to central mode behavior. We also obtained several additional recurrants, more than doubling the number of those already known in the literature.

ACKNOWLEDGMENTS

This work was supported by the Brazilian agencies CNPq, FAPERJ, FAPEMIG, CAPES, and PROPPi-UFF. One of the authors (O.F.A.B) acknowledges support from the Murdoch College of Science Research Program and a grant from the Research Corporation through Cottrell College Science Award No. CC5737.

[1] A. S. T. Pires, Helv. Phys. Acta **61**, 988 (1988).
[2] U. Brandt and J. Stolze, Z. Phys. B **64**, 327 (1986).
[3] M. Böhm and H. Leschke, J. Phys. A **25**, 1043 (1992); Physica A **199**, 116 (1993).
[4] O. F. de Alcantara Bonfim and G. Reiter, Phys. Rev. Lett. **69**, 367 (1992).
[5] J. Stolze, V. S. Viswanath, and G. Müller, Z. Phys. B-Cond. Matter **89**, 45 (1992).
[6] V. S. Viswanath and G. Müller, *The Recursion Method: Application to Many-Body Dynamics* (Springer, Berlin, 1994).
[7] M. H. Lee, J. Hong, and J. Florencio, Physica Scripta T **19B**, 498 (1987).
[8] U. Balucani, M. H. Lee, and V. Tognetti, Phys. Rep. **373**, 409 (2002).
[9] S. Hild, T. Fukuhara, P. Schauß, J. Zeiher, M. Knap, E. Demler, I. Bloch, and C. Gross, Phys. Rev. Lett. **113**, 147205 (2014).

[10] P. G. de Gennes, Solid State Commun. **1**, 132 (1963).
[11] R. Blinc and M. Ribaric, Phys. Rev. **130**, 1816 (1963).
[12] J. A. Plascak and S. R. Salinas, Phys. Stat. Sol. B **113**, 367 (1982).
[13] D. Bitko, T. F. Rosenbaum, and G. Aeppli, Phys. Rev. Lett. **77**, 940 (1996).
[14] Th. Niemeijer, Physica **36**, 377 (1967).
[15] U. Brandt and K. Jacoby, Z. Physik B **25**, 181 (1976).
[16] H. W. Capel and J. H. H. Perk, Physica A **87**, 211 (1977).
[17] J. Florencio and M. H. Lee, Phys. Rev. B **35**, 1835 (1987).
[18] R. J. Birgeneau, Phys. Rev. Lett. **26**, 718 (1971).
[19] M. T. Hutchings, Phys. Rev. B **5**, 1999 (1972).
[20] D. C. Johnston, J. W. Johnson, D. P. Goshorn, and A. J. Jacobson, Phys. Rev. B **35**, 219 (1987).
[21] M. Hagiwara, H. A. Katori, U. Schollwöck, and H. J. Mikeska, Phys. Rev. B **62**, 1051 (2000).
[22] P. Pfeuty, Ann. Phys. **57**, 79 (1970).
[23] R. Coldea, D. A. Tennant, E. M. Wheeler, E. Wawrzynska, D. Prabhakaran, M. Telling, K. Habicht, P. Smeibidl, and K. Kiefer, Science **327**, 177 (2010).
[24] A. Sommer, M. Ku, G. Roati, and M. W. Zwierlein, Nature (London) **472**, 201 (2011).
[25] M. Koschorreck, D. Pertot, E. Vogt, and M. Köhl, Nat. Phys. **9**, 405 (2013).
[26] A. B. Bardon, S. Beattie, C. Luciuk, W. Cairncross, D. Fine, N. S. Cheng, G. J. A. Edge, E. Taylor, S. Zhang, S. Trotzky, and J. H. Thywissen, Science **344**, 722 (2014).
[27] W. Selke, Phys. Rep. **170**, 213 (1988).
[28] H. Rieger and G. Uimin, Z. Phys. B **101**, 597 (1996).
[29] Paulo R. Colares Guimarães, J. A. Plascak, F. C. Sá Barreto, and J. Florencio, Phys. Rev. B **66**, 064413 (2002).
[30] A. Dutta and D. Sen, Phys. Rev. B **67**, 094435 (2003).
[31] S. Sen, C. N. Hoff, D. E. Kuhl, and D. A. McGrew, Phys. Rev. B **53**, 3398 (1996).
[32] X. J. Yuan, X. M. Kong, Z. B. Xu, and Z. Q. Liu, Physica A **389**, 242 (2010).
[33] A. Sur, D. Jasnow, and I. J. Lowe, Phys. Rev. B **12**, 3845 (1975); A. Sur and I. J. Lowe, *ibid.* **12**, 4597 (1975).
[34] K. Fabricius, U. Löw, and J. Stolze, Phys. Rev. B **55**, 5833 (1997).
[35] B. Boechat, C. Cordeiro, J. Florencio, F. C. Sá Barreto, and O. F. de Alcantara Bonfim, Phys. Rev. B **61**, 14327 (2000).
[36] M. H. Lee, Phys. Rev. B **26**, 2547 (1982); Phys. Rev. Lett. **49**, 1072 (1982).
[37] P. Grigolini, G. Grosso, G. Pastori Parravicini, and M. Sparpaglione, Phys. Rev. B **27**, 7342 (1983); M. Giordano, P. Grigolini, D. Leporini, and P. Marin, Phys. Rev. A **28**, 2474 (1983).
[38] M. H. Lee, I. M. Kim, and R. Dekeyser, Phys. Rev. Lett. **52**, 1579 (1984); M. H. Lee, Can. J. Phys. **61**, 428 (1983).
[39] M. H. Lee and J. Hong, Phys. Rev. Lett. **48**, 634 (1982); Phys. Rev. B **30**, 6756 (1984); M. H. Lee, J. Hong, and N. L. Sharma, Phys. Rev. A **29**, 1561 (1984).
[40] M. H. Lee, Phys. Rev. Lett. **51**, 1227 (1983).
[41] J. Florencio and M. H. Lee, Phys. Rev. A **31**, 3231 (1985).
[42] M. B. Yu, Physica A **398**, 252 (2014).
[43] S. Sen, Phys. Rev. B **44**, 7444 (1991); S. Sen, S. D. Mahanti, and Z. X. Cai, *ibid.* **43**, 10990 (1991).
[44] S. Sen and M. Long, Phys. Rev. B **46**, 14617 (1992); J. Appl. Phys. **73**, 5474 (1993).
[45] M. E. S. Nunes and J. Florencio, Phys. Rev. B **68**, 014406 (2003).
[46] M. Böhm, V. S. Viswanath, J. Stolze, and G. Müller, Phys. Rev. B **49**, 15669 (1994).
[47] M. H. Lee, J. Florencio, and J. Hong, J. Phys. A: Math. Gen. **22**, L331 (1989).
[48] S. Sen, Physica A **315**, 150 (2002).